

EXTREMELY HIGH ENERGY NEUTRINOS AND THEIR DETECTION

SHIGERU YOSHIDA

Institute for Cosmic Ray Research, University of Tokyo, Tokyo 188, Japan

AND

HONGYUE DAI, CHARLES C. H. JUI, AND PAUL SOMMERS

High Energy Astrophysics Institute, Department of Physics, University of Utah, Salt Lake City, UT 84112

Received 1996 August 19; accepted 1996 November 12

ABSTRACT

We discuss in some detail the production of extremely high energy (EHE) neutrinos with energies above 10^{18} eV. The most certain process for producing such neutrinos results from photopion production by EHE cosmic rays in the cosmic background photon field. However, using assumptions for the EHE cosmic-ray source evolution that are consistent with results from the deep QSO survey in the radio and X-ray range, the resultant flux of neutrinos from this process is not strong enough for plausible detection. A measurable flux of EHE neutrinos may be present, however, if the highest energy cosmic rays that have recently been detected well beyond 10^{20} eV are the result of the annihilation of topological defects which formed in the early universe. Neutrinos resulting from such decays reach energies of the grand unified theory scale, and collisions of superhigh-energy neutrinos with the cosmic background neutrinos initiate neutrino cascading, which enhances the EHE neutrino flux at Earth. We have calculated the neutrino flux including this cascading effect for either massless or massive neutrinos, and we find that these fluxes are conceivably detectable by air fluorescence detectors now in development. The neutrino-induced showers would be recognized by their starting deep in the atmosphere. We evaluate the feasibility of detecting EHE neutrinos this way using air fluorescence air shower detectors and derive the expected event rate. Other processes for producing deeply penetrating air showers constitute a negligible background.

Subject headings: cosmic microwave background — cosmic rays — cosmic strings — early universe — elementary particles — instrumentation: detectors

1. INTRODUCTION

It is well known that there exist extremely high energy particles in the universe with energies up to $\sim 10^{20}$ eV. How they are produced and how they propagate in the universe have been puzzles for a long time. Recent experiments suggest that these particles come from outside the Galaxy (Bird et al. 1993; Lawrence, Reid, & Watson 1991; Yoshida et al. 1995). More detailed understanding of their origin will require the detection of many more particles. It may also be necessary to observe the production process through other windows. Nucleons and nuclei lose their energies in less than ~ 100 Mpc through interactions with the cosmic microwave background (Greisen 1966; Zatsepin & Kuzmin 1996). Furthermore, intergalactic magnetic fields can bend their trajectories, masking their sites of origin. Gamma rays are even more limited in path length because of electron pair production when they collide with radio photons.

In this regard, neutrinos have uniquely advantageous characteristics: they can penetrate cosmological distances in the universe and their trajectories are not deflected because they have no electric charge. They carry information about extremely high energy (EHE) production processes, even in the early universe. It is therefore important to understand the possible processes for producing EHE neutrinos and to consider the possibilities for detecting the predicted flux resulting from several different models.

What mechanisms might produce EHE neutrinos? It has been pointed out that they should be produced at least by the Greisen mechanism: the decay of photopions produced by EHE cosmic-ray protons colliding with the cosmic thermal background photons (Greisen 1966; Hill & Schramm 1985; Yoshida & Teshima 1993). The detection of

Greisen neutrinos would itself supply firm evidence that EHE cosmic rays are coming from extragalactic space. The intensity of these neutrinos depends strongly on assumptions about the production of extragalactic EHE cosmic rays, and we need to make clear what kind of extragalactic sources might produce a detectable flux of Greisen neutrinos.

Another possibility has been proposed that would result in more copious EHE neutrinos. If monopoles and/or cosmic strings (so-called topological defects) were formed in symmetry-breaking phase transitions in the early universe, they may have produced EHE particles with energies up to the grand unified theory (GUT) scale (typically $\sim 10^{15}$ GeV) through their collapse or decay, with leptons and hadronic jets emitted from the supermassive so-called X-particles (Bhattacharjee, Hill, & Schramm 1992; Hill, Schramm, & Walker 1987). This hypothesis is of interest here because these jets are expected to produce many more neutrinos than nucleons, and the EHE neutrino flux might be detectable.

The detection of these EHE neutrinos is an interesting challenge. Currently, there is no detector designed specifically for detecting EHE neutrinos. However, an EHE neutrino could induce an electron in the terrestrial atmosphere, thereby initiating an electromagnetic air shower. Several detectors with huge acceptance of $\sim 10^4$ km² sr for giant air showers are now being constructed and/or planned, and we should not neglect the potential for EHE neutrino detection as a by-product of these detectors. The feasibility of EHE neutrino detection by giant air shower detectors must be evaluated together with a study of the possible background event types.

In this paper we analyze the production of EHE neutrinos and estimate their flux based on several different models. We also discuss prospects for EHE neutrino astrophysics which would result from detecting such a flux. The paper is organized as follows. Section 2 reviews Greisen neutrinos, which are produced by photopion production of the EHE cosmic-ray nucleons in intergalactic space. We present the possible flux for different assumptions about evolution of the EHE particle emitters and discuss the detection possibility. Some notes on neutrino emission from active galactic nuclei (AGN) are given in § 3. In § 4 we focus on the emission of EHE neutrinos from collapse or annihilation of topological defects (TDs) such as monopoles, cosmic strings, etc. Because neutrino cascades with the cosmological relic neutrinos have a significant effect on the resultant flux in this scenario (Yoshida 1994), we discuss the propagation of EHE neutrinos in detail for both massless and massive neutrinos in deriving the possible flux. We discuss in § 5 how to detect EHE neutrinos as deep air showers, using the air fluorescence detectors that are currently being constructed and planned. The event rate in these detectors for the TD scenario is also presented. The possibility of background events which could cause misidentification of neutrinos is considered in § 6. We summarize our conclusions in § 7.

2. THE GREISEN NEUTRINOS

Extremely high energy neutrinos above 10^{18} eV can be produced by photopion production between EHE cosmic-ray nucleons and the 2.7 K background photons during propagation in intergalactic space (Hill & Schramm 1985). Because neutrinos travel much longer distances than the cosmic-ray nucleons, the flux of these neutrinos depends heavily on assumptions about the evolution of the cosmic-ray sources, including cosmic-ray emission rates at high-redshift epochs (Yoshida & Teshima 1993, hereafter Paper I). The source evolution function, $\eta(t)$, is related to the cosmic-ray spectrum as follows:

$$J(E_{t_0}) = \int_{t_0}^{t_e} dt_e \eta(t_e) n(t_e) \left[\frac{R(t_e)}{R(t_0)} \right]^3 \times \int_{E_{t_0}} dE_{t_e} G(E_{t_e}, E_{t_0}, t_e) f(E_{t_e}). \quad (1)$$

Here $R(t_e)$ is the scale parameter of the universe at time t_e , $n(t_e)$ is the number density of sources at time t_e , E_{t_e} is the EHE cosmic-ray energy at the emission time t_e , E_{t_0} is the energy after propagation, and $f(E_{t_e})$ is the energy spectrum at the source. The term $G(E_{t_e}, E_{t_0}, t_e)$ gives the energy distribution at the present epoch t_0 for EHE cosmic rays that were input at time t_e with energy E_{t_e} , resulting from energy loss due to interactions with 2.7 K photons and adiabatic loss due to the expansion of the universe. This quantity plays the role of Green's function and is calculated by the transport equation for cosmic rays (Hill & Schramm 1985) or Monte Carlo simulation for propagation in the 2.7 K photon field (Yoshida & Teshima 1993). For astrophysical sources like radio galaxies or AGNs, we can consider the number of sources to be approximately conserved during the timescale we are interested in here. So equation (1) becomes

$$J(E_{t_0}) = n_0 \int_{t_0}^{t_e} dt_e \eta(t_e) \int_{E_{t_0}} dE_{t_e} G(E_{t_e}, E_{t_0}, t_e) f(E_{t_e}), \quad (2)$$

where n_0 is the number density of sources at present. If we assume $\eta(t)$ to be proportional to $(1+z)^m$, where z is the value of the redshift at time t , then equation (2) can be written as

$$J(E_{t_0}) dE_{t_0} = \frac{n_0 \eta_0}{H_0} \int_0^{z_{\max}} dz_e (1+z_e)^{m-5/2} \times \int_{E_{t_0}} dE_{t_e} G(E_{t_e}, E_{t_0}, z_e) f(E_{t_e}). \quad (3)$$

Here H_0 is the Hubble constant, and we assume an Einstein-de Sitter universe. In this expression, $m=0$ corresponds to the case of no evolution.

The neutrino flux becomes higher as the evolution parameter m and the “turn-on time” z_{\max} are increased. Figure 1 shows the spectrum of Greisen electron neutrinos under several assumptions for m and z_{\max} . These spectra are estimated by Monte Carlo simulation as in Paper I. The primary spectrum of cosmic-ray nucleons is assumed to be $\sim E^{-2}$ up to 10^{22} eV, though this assumption may be optimistic considering the proposed acceleration efficiency at radio galaxies (Biermann & Strittmatter 1987). However, even with these optimistic assumptions, the neutrino flux is found to be at most comparable to that of the EHE cosmic rays at around 10^{19} eV. Although the neutrino flux would be a good probe of m and z_{\max} pertaining to evolution of the EHE cosmic-ray production, detection of these fluxes with the current techniques is unlikely because of the low cross sections for neutrino interactions.

Let us consider the case of extremely strong source evolution here. If the primary spectrum of EHE cosmic rays is very hard and emissions at high-redshift epochs are responsible for the bulk of cosmic rays in intergalactic space, they would yield more neutrinos during their propagation. Figure 2 shows the expected neutrino spectrum for the case $m=7$ and $z_{\max}=5$ with a primary cosmic-ray spectrum $\sim E^{-1.5}$ calculated by the same Monte Carlo simulation as in Paper I. The neutrino flux exceeds the cosmic-ray flux by a factor of ~ 140 at around 10^{19} eV and may be detectable. However, we should note that these

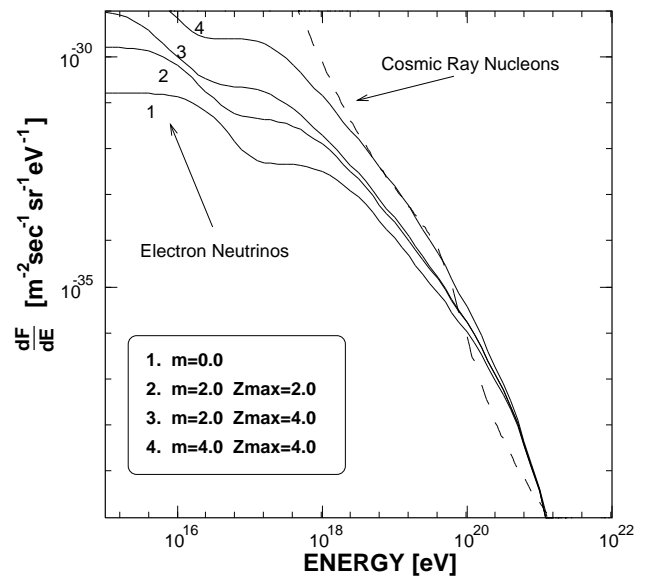


FIG. 1.—Energy spectrum of Greisen neutrinos under several assumptions of m and z_{\max} .

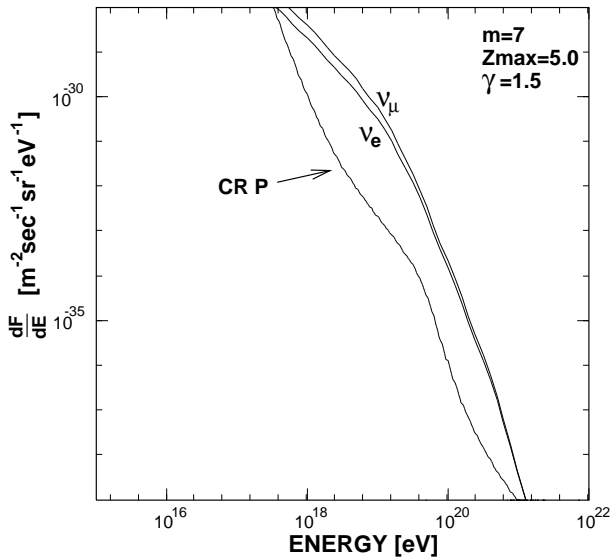


FIG. 2.—Energy spectrum of Greisen neutrinos for the strong source evolution case.

strong evolution assumptions would be inconsistent with the evolution of the luminosity functions of QSOs recently measured in the X-ray and radio range (Boyle et al. 1994; Dunlop & Peacock 1990). The deep sky survey with the *ROSAT* X-ray satellite found that $m = 3.25$ and $z_{\text{max}} = 1.6$ give the best fit to the observed data (Boyle et al. 1994). Therefore, if the powerful astrophysical sources like QSOs are the origin of the EHE cosmic rays as proposed by many authors (Rachen & Biermann 1993), it is hard to argue for a stronger evolution than this.

3. THE DIFFUSE NEUTRINOS FROM AGNs

Active galactic nuclei are possible acceleration sites for producing EHE cosmic rays, and the accelerated proton energy loss due to p-p and/or p- γ interactions in the AGN accretion disk or with UV photons in the associated jets are the dominant mechanisms for neutrino (and photon) production. Many authors have studied these processes to predict the possible neutrino fluxes (e.g., Szabo & Protheroe 1994; Stecker et al. 1991, 1992), mainly focusing on TeV and PeV neutrinos. Whether AGNs can produce EHE neutrinos with energies of 10 EeV or greater depends on the proton maximum energy. Radio-quiet AGNs, the most numerous class of AGNs, are not likely to produce EHE cosmic rays, while radio-loud AGNs might be able to produce EHE cosmic rays and neutrinos. Mannheim modeled the production mechanism of EHE neutrinos in the jets of radio-loud AGNs (Mannheim 1995) and found that the maximum neutrino energy reaches about 10 EeV. When the jet is pointing at the observer, particles accelerated in the moving jet plasma can gain an extra so-called Doppler factor (Mannheim 1993). An uncertainty in this model arises from the fact that we do not know how many radio-loud AGNs contribute to the bulk of energetic neutrinos and photons, and it would be difficult to give a reliable estimate of the normalization of the present-day neutrino flux. One possibility is to assume that the radio-loud AGNs are also responsible for the diffuse gamma-ray background above 100 MeV (Mannheim 1995). The increasing number of EGRET sources and the detection of

TeV photons from Mrk 421 and 501 (Punch 1992; Quinn et al. 1995) support this hypothesis, though these photon emissions could be driven not by π^0 decay but by inverse Compton scattering of energetic electrons without producing any neutrinos. Under the assumption that the energy flux of gamma rays emitted from radio-loud AGNs is comparable to the diffuse gamma-ray background, one obtains the EHE neutrino flux as $\sim 6 \times 10^{-33} \text{ m}^{-2} \text{ sr}^{-1} \text{ s}^{-1} \text{ eV}^{-1}$ at 10 EeV (Mannheim 1995), which is higher than the cosmic-ray flux by about a factor of 4. In this case the AGN neutrinos would dominate the Greisen neutrinos even in the EeV range. However, the predicted flux is still low and hard to detect, as will be described in § 5, and detection of TeV–PeV neutrinos from AGNs by underground neutrino telescopes is more feasible since the neutrino fluxes in this energy range are much higher and radio-quiet AGNs can also produce TeV–PeV neutrinos. PeV neutrinos from AGNs should be much easier to detect than EeV neutrinos because of the much higher expected fluxes.

4. EHE NEUTRINO EMISSION FROM TOPOLOGICAL DEFECTS

The possibility of producing EHE particles by the annihilation or collapse of TDs such as monopoles, cosmic strings, etc., has been proposed recently (e.g., Bhattacharjee et al. 1992; Hill et al. 1987). The maximum energy of the particles produced from TDs can reach the typical GUT energy scale. The energy trapped in the defects is released in the form of supermassive gauge bosons and Higgs bosons, which are usually referred to as X-particles. The decay of the X-particles can give rise to quarks, gluons, leptons, etc., which materialize into EHE nucleons, photons, and neutrinos with energies up to the GUT scale. This mechanism could be the origin of the highest energy cosmic-ray events well beyond 10^{20} eV detected by the Fly's Eye (Bird et al. 1995) and the Akeno Giant Air Shower Array (AGASA; Hayashida et al. 1994). Although we cannot exclude the possibility that these events could have originated at a nearby radio galaxy at an earlier time of strong activity if a strong magnetic field in the propagation space bent their trajectories (Elbert & Sommers 1995), the TD hypothesis appears to be a possible option because these extremely high energies would result from the direct production of particles from the decay of the supermassive X-particles without any acceleration mechanism, and the lack of any identifiable astrophysical sources near the arrival directions of these events is not a problem in this scenario because TDs are not necessarily associated with astrophysical sources (Sigl, Schramm, & Bhattacharjee 1994).

Among possible kinds of TDs, closed loops of cosmic strings have been studied most extensively as emitters of EHE cosmic rays. It has turned out that whether they would produce an observable cosmic-ray flux depends on the abundance of loops in the lowest oscillation state that collapse within 1 oscillating period before losing their trapped energies by gravitational wave radiation. This is a free parameter, and no definitive theory gives a strict limit for EHE cosmic-ray production by cosmic string loops.

Recently the production of EHE cosmic rays through a process that involves formation of metastable monopole-antimonopole bound states (monopolonium) and their subsequent annihilation has been studied (Bhattacharjee & Sigl 1995). In this scenario the measurable EHE cosmic-ray flux requires a fractional abundance of monopolonium of more

than $\sim 10^{-7}$ of the total monopole abundance. Although this requirement is not excluded by the Parker bound, the monopolonium fraction is quite speculative.

Therefore, the observation of EHE particles seems to be essential for testing whether these hypotheses are true or not. One prediction from the TD scenario is a high flux of EHE neutrinos, because the hadronic jets produced by the collapse of TDs would create many pions, which in turn emit neutrinos through their decays. The detection of the EHE neutrinos as well as the EHE gamma rays would support the hypothesis that the origin of EHE particles is related to GUTs.

The energies of EHE neutrinos produced by the collapse of TDs range up to the GUT energy scale ($\sim 10^{16}$ GeV), and their interactions with the cosmic thermal neutrinos (present temperature 1.9 K) produce a significant neutrino cascade (Yoshida 1994). The cascading increases the total EHE neutrino flux because a single neutrino from the X-decay can spawn multiple EHE neutrinos. Including this enhancement yields an EHE neutrino flux that is more likely to be detectable. In this chapter we derive the expected neutrino flux from TDs, taking into account the enhancement factor due to neutrino cascades. Our treatment of the propagation of neutrinos in the cosmic massless neutrino background field is described elsewhere (Yoshida 1994), but we also present a brief description here because it is essential for the flux estimation. Then we further discuss the neutrino cascading effect for the case of massive neutrino backgrounds. Finally, we calculate the differential neutrino flux for several assumptions for the masses of X-particles and neutrinos.

4.1. Propagation of EHE Neutrinos

4.1.1. Massless Neutrinos

Because energetic neutrinos expected in the TD scenario are likely to exceed 10^{14} GeV even at high redshifts of $z \geq 100$, collisions of these superhigh-energy neutrinos with the cosmic background neutrinos should occur. The cosmic background neutrinos follow the Fermi distribution:

$$\frac{dn}{dk_{bb}}(k_{bb}, T_v, z) = \frac{1}{2\pi^2 \hbar^3} \frac{k_{bb}^2}{\exp\{k_{bb}/[k_B T_v(1+z)]\} + 1}. \quad (4)$$

Here k_{bb} is the energy of the cosmic background neutrinos, T_v is the present blackbody temperature (1.9 K), k_B is Boltzmann's constant, and z is the redshift value at a given epoch.

The collision probability between EHE neutrinos and the thermal background neutrinos is given by (Yoshida 1994)

$$\frac{dF}{dt dE_{rec}}(E_v, z) = \frac{1}{4\pi} \int ds \frac{d\sigma}{dE_{rec}}(s) \times \int d\Omega (1 + \cos \theta) \frac{dn}{dk_{bb}}(k_{bb}, T_v, z) \frac{dk_{bb}}{ds}, \quad (5)$$

where θ is the collision angle between the EHE neutrino and the background neutrino; E_v is the EHE neutrino energy at the epoch with redshift z ; s is the Lorentz invariant parameter, which can be written in the cosmic-ray laboratory frame (CRLF) as

$$s = 2E_v k_{bb}(1 + \cos \theta); \quad (6)$$

σ is the cross section for the interaction; and E_{rec} is the recoil energy of collision particles such as electrons, muons, taus, quarks, and neutrinos. Their decays or hadronizing

process would produce neutrinos and further contribute to the neutrino cascade. The main interactions in the neutrino cascade are the following: (a) s-channel Z_0 exchange, (b) t-channel W^\pm exchange, (c) t-channel Z_0 exchange, (d) interference between (a) and (b), (e) interference between (a) and (c), and (f) interference between (c) and u-channel Z_0 exchange. The most important ones are channel a, which has resonance behavior, and channel b, which becomes important above the resonance energy for coupling of neutrinos with different flavors. The cross sections for these channels are, respectively, written as

$$\frac{d\sigma}{d \cos \theta^*} = \frac{G^2 s}{4\pi} \frac{M_z^2}{(s - M_z)^2 + M_z^2 \Gamma_z^2} \times [g_L^2(1 + \cos \theta^*)^2 + g_R^2(1 - \cos \theta^*)^2], \quad (7)$$

$$\frac{d\sigma}{d \cos \theta^*} = \frac{G^2 s}{4\pi} \frac{M_w^2(1 + \cos \theta^*)^2}{[(s/2)(1 - \cos \theta^*) + M_w^2]^2}, \quad (8)$$

where G is the weak interaction coupling constant; θ^* is the rotation angle of the collision in the center-of-momentum system; M_z and M_w are the masses of Z_0 and W^\pm , respectively; Γ_z is the decay width of Z_0 ; and g_L and g_R are the left-handed and right-handed coefficients, respectively. Although these two channels are the main contributors to the cascade, we take into account also the other channels c-f. Since the energy of the recoil particles, E_{rec} , is related to θ^* through a Lorentz transformation, $d\sigma/dE_{rec}$ can be calculated from $d\sigma/d\theta^*$.

The number of produced neutrinos per unit length per unit energy is given by

$$\frac{dN_{j \rightarrow i}}{dE_{v,i} dL} = \int dE_{rec} \frac{dn}{dE_{v,i}}(E_{v,i}, E_{rec}) \frac{dF}{dL dE_{rec}}(E_{v,j}, z), \quad (9)$$

where i and j denote the types of neutrinos like ν_e , ν_μ , and ν_τ and $dn/dE_{v,i}$ is the energy distribution of the secondary neutrinos produced by the recoil particle. For elastic collisions, these will be delta functions, and for the produced muons and taus, they can be derived by the decay matrix elements (Gaisser 1990). Quarks fragment and produce jets of hadrons that emit neutrinos through their decays, so $dn/dE_{v,i}$ can be gotten by convolution of the hadronic fragmentation spectrum with the hadron decay spectrum. The fragmentation spectrum can be written as (Hill et al. 1987)

$$\frac{dN_h}{dx} \simeq 0.08 \exp \left[2.6 \sqrt{\ln \left(\frac{1}{x} \right)} \right] (1-x)^2 \left[x \sqrt{\ln \left(\frac{1}{x} \right)} \right]^{-1}. \quad (10)$$

Here, $x = E/E_{jet}$ is the energy of a hadron in the jet and N_h is the number of hadrons with fraction x of the energy in the jet E_{jet} . We assume that 97% of the hadrons in the jet are pions (Bhattacharjee et al. 1992).

Then we can write the transport equation of EHE neutrinos using equation (9) as follows (Yoshida 1994):

$$\begin{aligned} \frac{dN_i}{dL}(E_{v,i}, z) &= -\frac{N_i(E_{v,i}, z)}{\lambda_i(E_{v,i}, z)} \\ &+ \sum_{j=\nu_e, \nu_\mu, \nu_\tau} \int_{E_{v,i}}^{E_{v,i}^{\max}} dE'_{v,j} N_j(E'_{v,j}, z) \frac{dN_{j \rightarrow i}(E'_{v,j}, E_{v,i}, z)}{dE_{v,i} dL} \\ &+ \frac{d}{dE_{v,i}} [H_0(1+z)^{3/2} E_{v,i} N_i(E_{v,i}, z)], \quad i = \nu_e, \nu_\mu, \nu_\tau. \end{aligned} \quad (11)$$

Here λ_i is the mean free path that is calculated by integrating equation (5) over E_{rec} and s , H_0 is the Hubble constant, and the third term on the right-hand side of equation (11) expresses the adiabatic loss due to the expansion of the universe. Numerical solution of equation (11) gives the energy distribution of EHE neutrinos after their propagation.

Figure 3 shows an example of the EHE neutrino energy distribution in the neutrino cascade. One can see the secondary bulk of lower energy neutrinos. This is mainly contributed by the hadronic jet that channel a produces at around the Z_0 resonance energy ($\sim 3 \times 10^{15}$ GeV). You will see that this bulk enhances the final flux of neutrinos.

4.1.2. Massive Neutrinos

It is well known that invoking a small mass for cosmological background neutrinos might resolve the dark matter problem. Comparing the cosmological mass density and the neutrino density gives a constraint on the masses of stable neutrinos as (Bludman 1992)

$$\sum_{\nu_e, \nu_\mu, \nu_\tau} m_\nu = 92\Omega_0 h^2 \text{ eV}, \quad (12)$$

where Ω_0 is the total cosmological mass density normalized by the critical density of the universe and the Hubble constant is $H_0 = 100 h \text{ km s}^{-1} \text{ Mpc}^{-1}$. The mass density Ω_0 is related to the Hubble constant H_0 and the present age of the universe t_0 :

$$H_0 t_0 = \begin{cases} -\frac{1}{\Omega_0 - 1} + \frac{\Omega_0}{(\Omega_0 - 1)^{3/2}} \tan^{-1} (\Omega_0 - 1)^{1/2}, & \text{closed universe,} \\ -\frac{1}{\Omega_0 - 1} - \frac{\Omega_0}{(1 - \Omega_0)^{3/2}} \tanh^{-1} (1 - \Omega_0)^{1/2}, & \text{open universe,} \\ \frac{2}{3}, & \text{flat universe.} \end{cases} \quad (13)$$

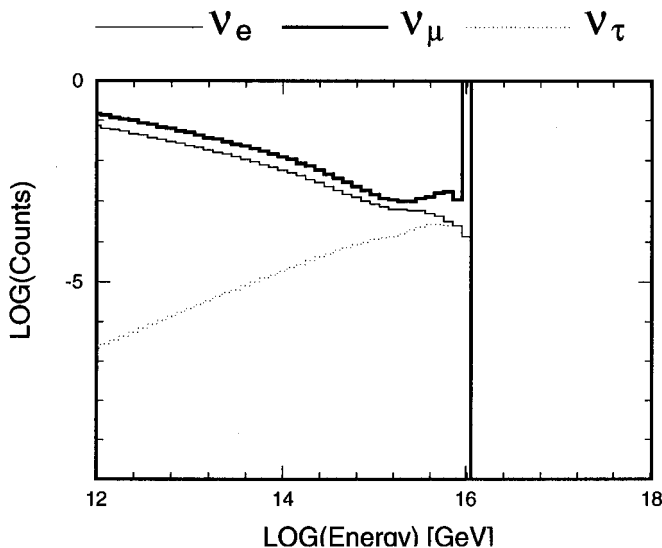


FIG. 3.—Energy distribution of EHE neutrinos in the cascade after propagation through 1 Gpc. Primary input spectrum is monochromatic energy distribution of 10^{16} GeV muon neutrinos.

The age of the universe can be estimated from measured ages of star clusters (Sandage & Cacciari 1990) to be $t_0 = 13\text{--}17$ Gyr. Allowing $0.5 \leq h \leq 1.0$, equation (13) and t_0 give

$$\Omega_0 h^2 \leq 0.038\text{--}0.255, \quad (14)$$

and the neutrino mass limitation is given by

$$\sum_{\nu_e, \nu_\mu, \nu_\tau} m_\nu \leq 3.5\text{--}23 \text{ eV}. \quad (15)$$

Thus, for example, $m_{\nu_e} = m_{\nu_\mu} = m_{\nu_\tau} = 1 \text{ eV}$ are still allowed by this somewhat strict constraint. For simplicity in the following discussion, masses of neutrinos are assumed to be the same for all flavors.

If the rest-mass energy of cosmological background neutrinos is much higher than their blackbody temperature, their energy distribution is effectively monochromatic. Thus, the probability of collision between EHE neutrinos and the cosmic background neutrinos, equation (5), becomes

$$\frac{dF}{dt dE_{\text{rec}}} (E_\nu, z) \simeq (1+z)^3 n_0 \left. \frac{d\sigma}{dE_{\text{rec}}} \right|_{s=2m_\nu E_\nu}, \quad (16)$$

where n_0 is the number density of the background neutrinos in the present universe ($\sim 108 \text{ cm}^{-3}$ for $\nu + \bar{\nu}$ in each flavor). We get the mean free path by integrating equation (16):

$$\lambda(E_\nu, z) \simeq (1+z)^{-3} (n_0 \sigma|_{s=2m_\nu E_\nu})^{-1}. \quad (17)$$

Figure 4 shows the mean free path obtained by equation (17). The Z_0 resonance effect on the cross section for channel a (see eq. [7]) creates the bump at around

$$E_\nu|_{\text{resonance}} = \frac{M_Z^2}{2m_\nu} = 4 \times 10^{12} \left(\frac{m_\nu}{1 \text{ eV}} \right)^{-1} \text{ GeV}. \quad (18)$$

Above this energy region, t - W^\pm exchange (see eq. [8]) become the dominant channels.

Numerical solution of the transport equation, equation (11), together with equations (9), (16), and (17) give the EHE neutrino energy distribution propagating in the massive background neutrino field. Figure 5 shows the energy dis-

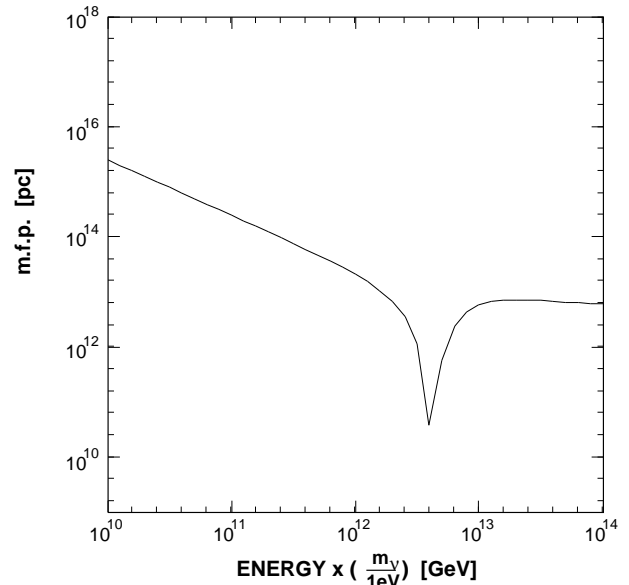


FIG. 4.—Mean free path of EHE neutrinos in the massive cosmological neutrino backgrounds at present epoch.

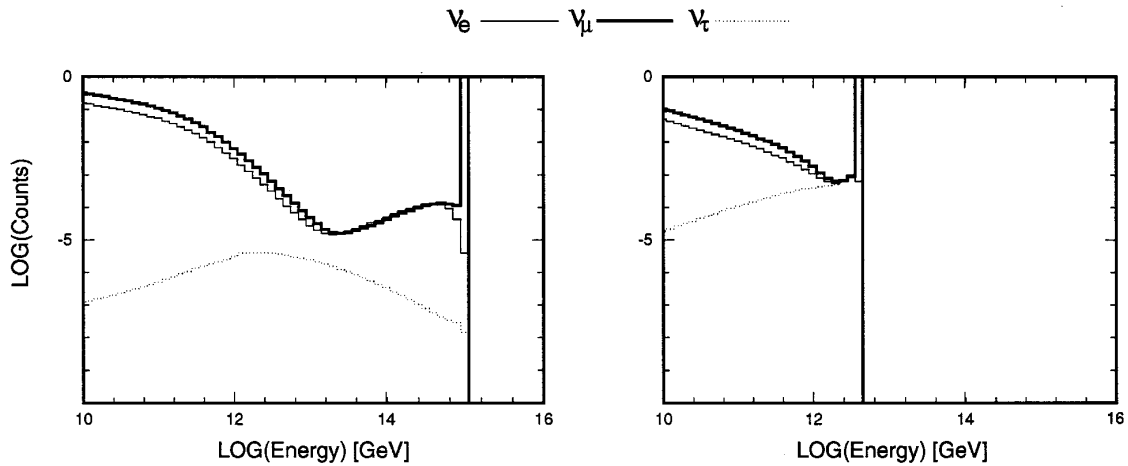


FIG. 5.—Energy distribution of EHE neutrinos after propagation through 1 Gpc in the background neutrinos with $m_\nu = 1$ eV. Primary input spectra are monochromatic energy distributions of 10^{15} GeV and 3×10^{12} GeV muon neutrinos, respectively.

tribution of EHE neutrinos propagating in the background neutrino field with $m_\nu = 1$ eV. The transition of the secondary neutrino energy distribution is found at around 10^{13} GeV because the main contribution for the bulk of the lower energy neutrinos is the decay of pions in the hadronic jets that are emitted through the interaction of s - Z_0 exchange, while the secondary neutrinos with higher energies come mainly from the ν - $\bar{\nu}$ coupling through the W^\pm exchange.

Figure 6 shows the expected spectral shape from a single source of EHE neutrinos. The sharp dip appears because of the Z_0 resonance behavior as described above. Creation of this dip has been pointed out by Roulet (1993) using simple analysis considering only the absorption effect by the background neutrinos. We also find a slight enhancement of the flux at lower energy. This enhancement created by the bulk of the secondary neutrinos will play an important role in studying the final flux of neutrinos from TDs.

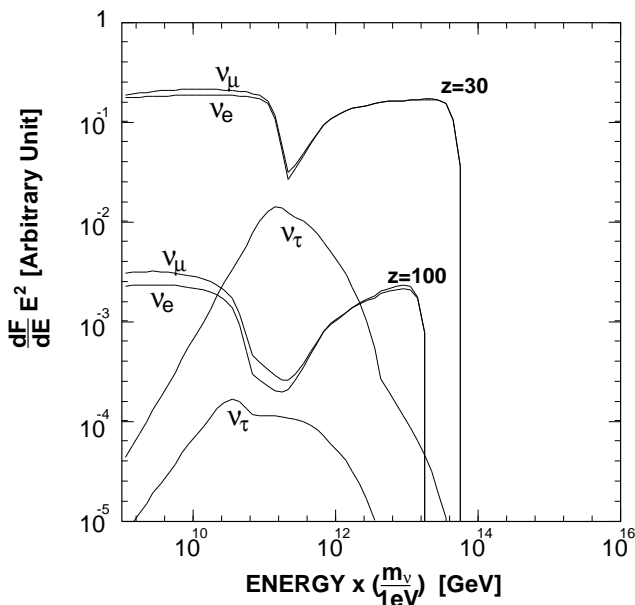


FIG. 6.—Energy spectra of EHE neutrinos propagating in the massive cosmological background neutrino field. The primary spectra are assumed to be $\sim E^{-2}$.

4.2. Flux of EHE Neutrinos

The release rate of the X-particles by collapse of cosmic string loops or monopoles (Bhattacharjee & Sigl 1995) is given by

$$\frac{dn_X}{dt} = \kappa t^{-3}, \quad (19)$$

where κ is determined mainly from the abundance of the string loops in the lowest oscillation state or the abundance of monopoles and the X-particle mass, all of which are unknown. We get the final flux of EHE neutrinos after propagating in the cosmic background neutrinos using equation (1):

$$J(E_{t_0}) = \int^{t_0} dt_e \frac{dn_X}{dt_e} \left[\frac{R(t_e)}{R(t_0)} \right]^3 \int_{E_{t_0}} dE_{t_e} G(E_{t_e}, E_{t_0}, t_e) f(E_{t_e}). \quad (20)$$

Green's function G is calculated by the transport equation, equation (11). Because the primary neutrinos are produced by decay of the pions in the hadronic jets from X-particle decay, the primary neutrino spectrum $f(E_{t_e})$ is given by the convolution of the hadronic fragmentation spectrum, equation (10), and the pion-muon decay spectrum (Yoshida 1994; Bhattacharjee et al. 1992; Bhattacharjee & Sigl 1995). We assume the jet energy is $m_X/2$ and 97% of hadrons in the jet are pions as in the previous calculations (e.g., Bhattacharjee et al. 1992). It should be noted that the EHE neutrino spectrum is not sensitive to the rate of annihilations in the early radiation-dominated universe ($z > 10^4$), since any neutrinos produced then would have cascaded to lower energies. It is sensitive, however, to the evolution described by equation (19) for $z > 100$ both because of the high TD annihilation rate at early times and because the target background neutrinos then had higher energy and greater density.

Because the value of κ in equation (19) is uncertain, the observed flux of EHE cosmic rays sets the normalization. If the extragalactic component of EHE cosmic rays dominates above around $10^{18.5}$ – 10^{19} eV, where the change of the spectral slope has been observed (Bird et al. 1994; Nagano et al. 1992; Yoshida et al. 1995), it is consistent to assume that the cosmic rays above about 5×10^{19} eV are mainly from the collapse of TDs. This assumption gives an intensity of protons from TDs that is lower than the observed flux over

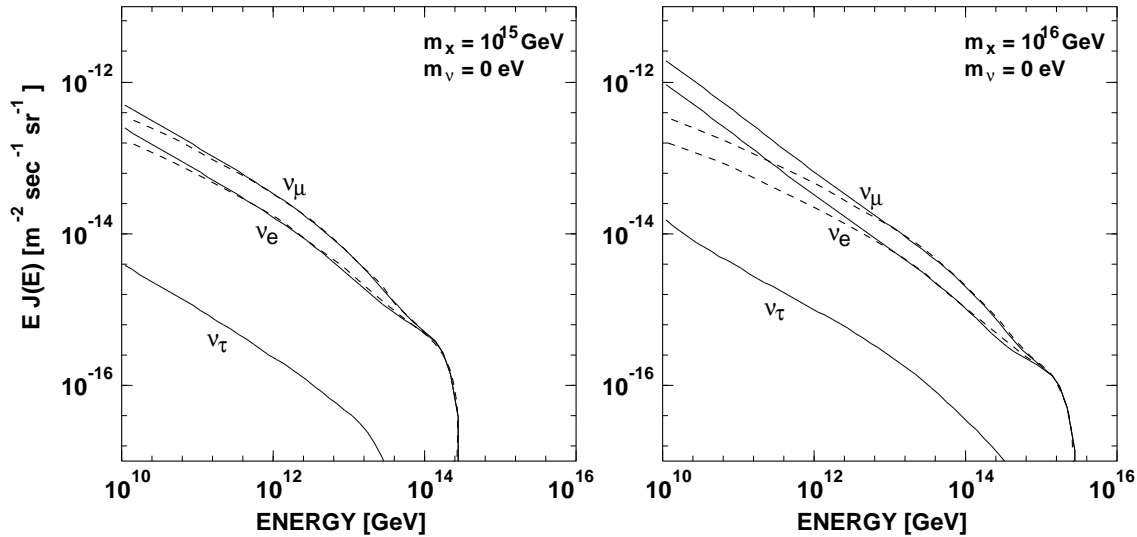


FIG. 7.—Differential flux of EHE neutrinos from the collapse of the cosmic string loops or monopolonium. All neutrinos are assumed to be massless particles. *Dashed curves*: Results calculated if only the energy loss due to the expansion of the universe is considered.

the whole energy range, and the superhigh energetic events observed by Fly’s Eye (Bird et al. 1995) and AGASA (Hayashida et al. 1994) well beyond 10^{20} eV can be explained as gamma rays from TD annihilations (Sigl et al. 1994; Bhattacharjee & Sigl 1995; Chi et al. 1993). Here we use the normalization obtained from the assumption that the cosmic-ray intensity at 5×10^{19} eV observed by Fly’s Eye (Bird et al. 1994) is contributed by protons (and neutrons) from TDs. This normalization is constrained by their contribution to the diffuse gamma-ray background for $E_\gamma \simeq 200$ MeV but not completely ruled out yet (Sigl et al. 1995). The recent reevaluation of the γ -ray flux (Sigl, Lee, & Coppi 1996) demonstrates that the normalization is allowed for extragalactic magnetic field strengths of $\leq 10^{-11}$ G, which are consistent with current estimates (Kronberg 1994).

Figures 7 and 8 show the expected flux from cosmic string loops or monopolonium for the case of massless neutrinos and those with 1 eV mass, respectively. It is found that the secondary neutrinos produced in the neutrino cascade enhance the intensity below $\sim 10^{20}$ eV. For the massive neutrino case, the sharp dip structure appearing in the spectrum from each source as shown in Figure 6 suppresses the intensity at around the Z_0 resonance energy expressed by equation (18). The flux at the lower energies, however, is enhanced by the cascading effect.

The fluxes obtained here are much higher than the Greisen neutrinos discussed in § 2. The integral flux above 10^{19} eV is listed in Table 1. We should note that the flux estimate has an uncertainty of about a factor of 2 due to the

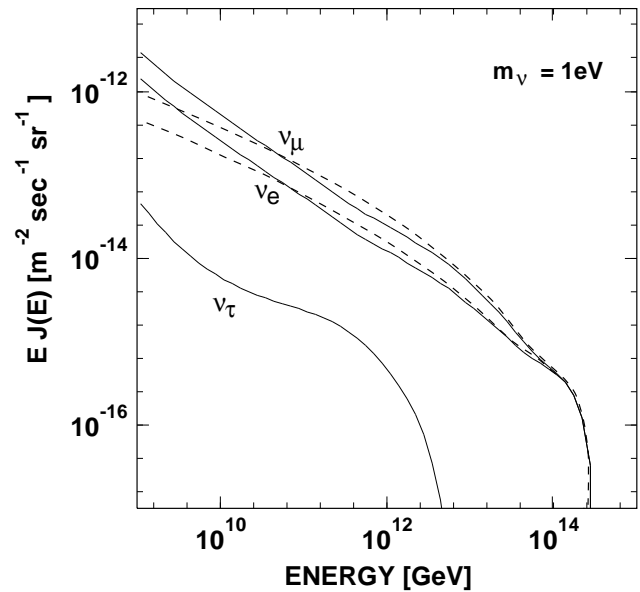


FIG. 8.—Differential flux of EHE neutrinos from the collapse of the cosmic string loops or monopolonium. Masses of all neutrinos are assumed to be 1 eV. *Dashed curves*: Results calculated if only the energy loss due to the expansion of the universe is considered.

poor cosmic-ray statistics at 5×10^{19} eV and possible systematics in the cosmic-ray energy estimation (Bird et al. 1994; Yoshida et al. 1995). The flux depends on the assumption of the hadronic fragmentation spectrum because the

TABLE 1
INTEGRAL NEUTRINO FLUX ABOVE 10^{19} eV FOR THE DIFFERENT ASSUMPTIONS

| NEUTRINO | FLUX | | | OBSERVED COSMIC RAYS |
|-----------------|---------------------------------------|---------------------------------------|---------------------------------------|-----------------------|
| | $m_x = 10^{16}$ GeV $m_\nu = 0$ eV | $m_x = 10^{15}$ GeV $m_\nu = 0$ eV | $m_x = 10^{15}$ GeV $m_\nu = 1$ eV | |
| ν_e | 1.4×10^{-12} | 4.4×10^{-13} | 3.8×10^{-13} | 1.4×10^{-14} |
| ν_μ | 2.8×10^{-12} | 8.9×10^{-13} | 7.7×10^{-13} | ... |

NOTE.—All values are measured in $m^{-2} s^{-1} sr^{-1}$.

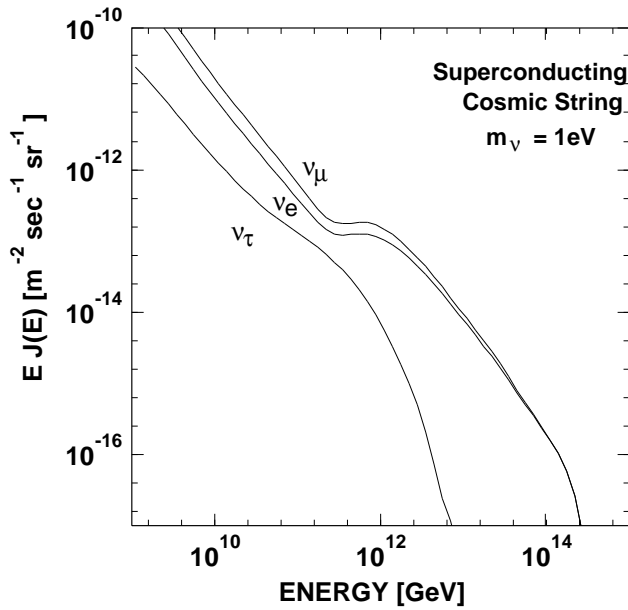


FIG. 9.—Differential flux of EHE neutrinos from saturated superconducting cosmic string loops. Masses of all neutrinos are assumed to be 1 eV.

hadronic jets play an important role in determining both the primary spectrum and the flux enhancement by neutrino cascading. It has been pointed out (Chi et al. 1993) that the fragmentation spectrum could be steeper than equation (10), giving $\sim E^{-1.3}$, and the final flux could be higher by more than a factor of 10. Thus the fluxes we present here could still be conservative.

There is another potential TD that could be a source of EHE cosmic rays: the saturated superconducting cosmic string loops (SCS) (Hill et al. 1987). Although this hypothesis might have several difficulties in producing EHE particles due to constraints by the low-energy γ -ray backgrounds and the light-element abundances in the universe (Sigl et al. 1995), strong evolution could give a high flux of neutrinos. The release rate of the X-particle is $\sim t^{-4}$ ($\sim t^{-3}$ for the ordinary string loops and monopoles as expressed in eq. [19]), and the neutrinos at earlier epochs mainly contribute to the bulk of EHE neutrinos. A massive neutrino background would provide an especially interesting possibility. Figure 9 shows the expected EHE neutrino spectrum from SCS for a neutrino mass of 1 eV. The dip structure as seen in Figure 6 is not smeared even in summing over the EHE neutrinos from SCS at different epochs according to equation (20), because of the strong evolution. The neutrino spectrum expected from this scenario would have this indicator of the neutrino mass.

5. DETECTION OF THE EHE NEUTRINOS

The fluxes calculated above are in the range 10–30 vs $\text{km}^{-2} \text{yr}^{-1} \text{sr}^{-1}$ above 10^{19} eV, and their detection requires a detector of huge aperture considering the low neutrino cross sections. The standard-type underground neutrino telescopes, which observe long-range upward-going muons with effective areas of 0.1 km^2 or smaller, would not be capable of EeV neutrino detection (Gandhi et al. 1995). An alternative detection method is to search for extensive air showers (EAS) initiated by electrons produced by neutrinos through the charged current process $\nu_e + N \rightarrow e + X$.

Showers developing deep in the atmosphere must be produced by penetrating particles. The Fly's Eye experiment searched for such an event to get an upper bound on the EHE neutrino flux (Baltrusaitis et al. 1985; Emerson 1992). The predicted fluxes are still lower than this bound by about a factor of 10. There are large new detectors for measuring EHE cosmic-ray air showers using air fluorescence that are now under construction or development. These will have large enough apertures to have the potential to search for EHE neutrinos (HiRes collaboration 1993; Teshima et al. 1992). These detectors can reconstruct the EAS development as a function of atmospheric depth with better than 30 g cm^{-2} resolution and easily distinguish normally developing showers from deeply penetrating showers.

The interaction length of cosmic-ray hadrons and γ -rays is 50–100 g cm^{-2} near 10^{19} eV. Thus the probability of these particles initiating EAS at deeper than 2000 g cm^{-2} is less than 2×10^{-9} , so any shower starting that deep in the atmosphere would be a candidate neutrino event. The event rate of deeply penetrating showers (DPS) induced by EHE neutrinos is given by

$$\frac{dN}{dt} (\geq E_{\nu_e}) = N_A \int_{E_{\nu_e}}^{\infty} dE'_{\nu_e} J(E'_{\nu_e}) \times \int_0^{E_{\nu_e'}} dE_e \frac{d\sigma_{\nu_e}}{dE_e}(E'_{\nu_e}) \int d\Omega (X_{\Omega} - 2000 \text{ g cm}^{-2}) A(\Omega), \quad (21)$$

where σ_{ν_e} is the cross section of the charged current process with the nucleon, E_e is the energy of the produced electrons, N_A is Avogadro's number, X_{Ω} is the slant depth of the atmosphere for the solid angle Ω , and $A(\Omega)$ is the acceptance of the air fluorescence detector for deeply penetrating showers.

The charged current cross section in this energy region has not been measured and could be uncertain. The observed small- x behavior of the QCD structure functions, however, gives an estimate of the cross section without large ambiguity, and it turns out that the cross section is not saturated because of the evolution of the QCD structure functions (e.g., Mackey & Ralston 1986; Quigg, Reno, & Walker 1986; Gaisser & Stanev 1985). Figure 10 shows the calculated total cross section of $\nu + N \rightarrow l^{\pm} + X$. The increase in the cross section is favorable for EHE neutrino detection.

The DPS acceptance, $A(\Omega)$ in equation (21), is estimated by Monte Carlo detector simulations. For discussing the sensitivity for neutrino detection, it is useful to define the “effective aperture” that is folded with the cross section:

$$D_{\nu}(E_{\nu_e}) = N_A \int_0^{E_{\nu_e}} dE_e \frac{d\sigma_{\nu_e}}{dE_e}(E_{\nu_e}) T(E_e), \quad (22)$$

$$T(E_e) = \int d\Omega (X_{\Omega} - 2000 \text{ g cm}^{-2}) A(\Omega, E_e). \quad (23)$$

The term $T(E_e)$ represents the effective aperture column density ($\text{km}^2 \text{sr g cm}^{-2}$) of the detector for the DPS as a function of energy of the neutrino-induced electrons. Then the event rate is estimated from equation (21) as

$$\frac{dN}{dt} (\geq E_{\nu_e}) = \int_{E_{\nu_e}}^{\infty} dE'_{\nu_e} J(E'_{\nu_e}) D_{\nu}(E'_{\nu_e}). \quad (24)$$

Monte Carlo detector simulation can calculate the effective target volume $T(E_e)$, but we shall give a rough estimate

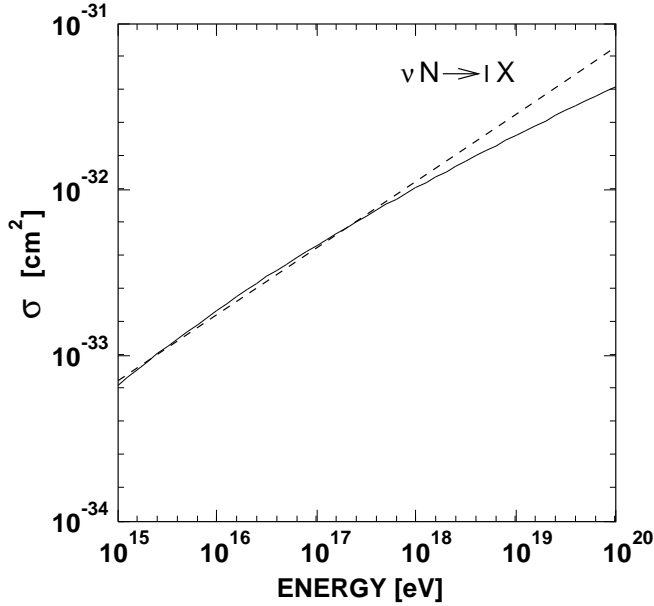


FIG. 10.—Cross section of the charged current process $\nu + N \rightarrow l^+ + X$ calculated by Mackey & Ralston. *Dashed curve*: Obtained by the recent reevaluation of parton distribution measured by HERA.

with a simple analytic calculation first. A phototube in the telescope is useful in an event only if it collects more air fluorescence light emitted from the shower track than the fluctuation of night-sky background light during its integration time t_{gate} . The expected air fluorescence signal is given by

$$N_{\text{ph}} = \frac{A_{\text{mir}} N_e Q}{4\pi r_p^2} \exp\left(-\frac{r_p}{r_0}\right) e_{\text{eff}} r_p \Delta\theta, \quad (25)$$

where r_p is the shower's impact parameter, A_{mir} is the area of a mirror in the telescope, N_e is the number of electrons in the shower cascade viewed by that phototube, r_0 is the extinction length of light due to the atmospheric scattering, e_{eff} is the fluorescence light yield from an electron (photons per meter), $\Delta\theta$ is the phototube pixel size, and Q is the quantum efficiency of the phototube. The background light is given by

$$N_{\text{BG}} = n_{\text{NB}} t_{\text{gate}} A_{\text{mir}} Q (\Delta\theta)^2, \quad (26)$$

where n_{NB} is the night-sky photon intensity and t_{gate} is the gate time for collecting signal. Then the signal-to-noise ratio n_{th} gives the threshold shower electron size for triggering a channel as a function of r_p as follows:

$$N_{e,\text{th}} = n_{\text{th}} 4\pi r_p \exp\left(\frac{r_p}{r_0}\right) e_{\text{eff}}^{-1} \sqrt{\frac{n_{\text{NB}} t_{\text{gate}}}{A_{\text{mir}} Q}}. \quad (27)$$

To an accuracy of 35%, this equation can be written as

$$\begin{aligned} \log N_{e,\text{th}} &= 7.54 + \left(\frac{r_0}{8 \text{ km}}\right)^{-4/5} 8.23 \times 10^{-2} \left(\frac{r_p}{1 \text{ km}}\right) \\ &+ \log \left[n_{\text{th}} \left(\frac{r_0}{8 \text{ km}}\right) \left(\frac{e_{\text{eff}}}{4 \text{ m}^{-1}}\right)^{-1} \right. \\ &\quad \left. \times \left(\frac{R_{\text{mir}}}{1 \text{ m}}\right)^{-1} \sqrt{\left(\frac{n_{\text{NB}}}{10^6 \text{ m}^{-2} \text{ sr}^{-1} \mu\text{s}^{-1}}\right) \left(\frac{t_{\text{gate}}}{5 \mu\text{s}}\right)} \right], \end{aligned} \quad (28)$$

where R_{mir} is the radius of the telescope mirror and Q is assumed to be 30%.

The atmospheric slant width during which the shower cascade contains more electrons than this threshold size $N_{e,\text{th}}$ can be considered as a target depth for showers to trigger a detector with almost 100% efficiency. The longitudinal development of an electromagnetic air shower is described by the Greisen formula (Greisen 1956), and we obtain the following expression for the target numerically:

$$X_t^{100\%} = X_t(N_e \geq N_{e,\text{th}}) = 100(-\eta^2 - 8\eta + 2) \text{ g cm}^{-2}, \quad (29)$$

$$\eta = \log(N_{e,\text{th}}) - \log\left(\frac{E_e}{1 \text{ GeV}}\right).$$

Using equation (28), η can be written as a function of r_p and thus $X_t^{100\%}$ is a function of E_e and r_p . We should remark that requiring $X_t^{100\%} \geq 0$ leads to a maximum shower distance at which the telescope will trigger:

$$r_p^{\text{max}} = 12.15 \left(\frac{r_0}{8 \text{ km}}\right)^{4/5} f \text{ km}, \quad (30)$$

where

$$\begin{aligned} f &= 2.7 + \log\left(\frac{E}{10^{19} \text{ eV}}\right) \\ &- \log \left[n_{\text{th}} \left(\frac{r_0}{8 \text{ km}}\right) \left(\frac{e_{\text{eff}}}{4 \text{ m}^{-1}}\right)^{-1} \right. \\ &\quad \left. \times \left(\frac{R_{\text{mir}}}{1 \text{ m}}\right)^{-1} \sqrt{\left(\frac{n_{\text{NB}}}{10^6 \text{ m}^{-2} \text{ sr}^{-1} \mu\text{s}^{-1}}\right) \left(\frac{t_{\text{gate}}}{5 \mu\text{s}}\right)} \right]. \end{aligned} \quad (31)$$

At 10^{19} eV with $n_{\text{th}} = 2$ (2σ deviation), $r_p^{\text{max}} \sim 29$ km for the detectors under development operating in a desert atmosphere.

Now we can calculate the effective aperture column density, $T(E_e)$, as

$$T(E_e) = 2\pi \int d \cos \theta \int dr_p r_p X_t^{100\%}(r_p, E_e) \int d\chi. \quad (32)$$

Here we assume that our detector has azimuthally symmetric sensitivity. For integration over zenith angle θ , and azimuthal angle around the r_p axis χ , we need to take into account the limit that the shower must be deeper than 2000 g cm^{-2} :

$$X_0 \exp\left(-\frac{r_p \sin \theta \sin \chi}{h}\right) \geq 2000 \cos \theta \text{ g cm}^{-2}. \quad (33)$$

Here X_0 is the atmospheric vertical depth at the detector ($\sim 1000 \text{ g cm}^{-2}$) and h is the atmospheric scale height (~ 7.5 km). After introducing some approximations, we finally obtained

$$\begin{aligned} T(E_e) &\simeq 1.1 \times 10^5 \left(\frac{h}{8.4 \text{ km}}\right) \left(\frac{r_0}{8 \text{ km}}\right)^{4/5} f^2 \\ &- 7 \times 10^4 \left(\frac{h}{8.4 \text{ km}}\right)^2 \text{ km}^2 \text{ sr g cm}^{-2}. \end{aligned} \quad (34)$$

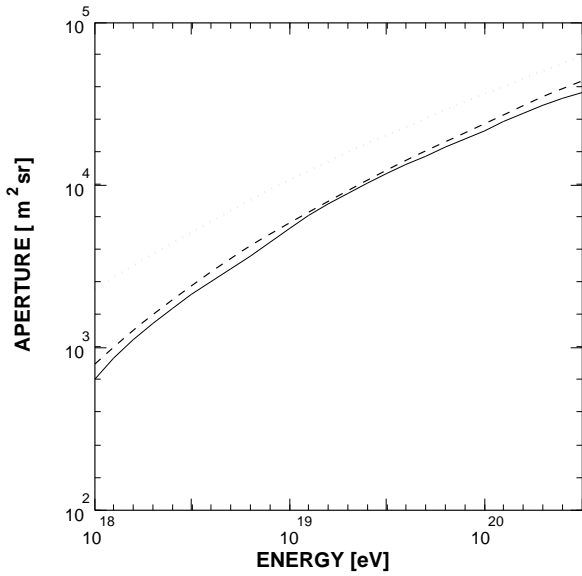


FIG. 11.—Effective aperture for EHE electron neutrinos expected for the HiRes and the Telescope Array detector performances. *Solid curve*: Results obtained by the HiRes Monte Carlo simulation. *Dashed curve*: Results obtained by the analytical formula with the HiRes detector parameters. *Dotted curve*: Corresponds to the aperture of the Telescope Array which was also calculated by the analytical formula.

Equations (22), (31) and (34) give the effective neutrino aperture for a detectors with mirror radius R_{mir} and integration time t_{gate} .

We can confirm these estimates using the Monte Carlo program for the High Resolution Fly’s Eye (HiRes), now being constructed at Dugway, Utah (HiRes Collaboration 1993). HiRes has two eyes separated by 12.6 km and 1° pixel size. We use the Monte Carlo code developed for estimate of the HiRes aperture taking into account the detector performance and atmospheric scattering (Dai 1993).

Figure 11 shows the effective aperture for the HiRes detector obtained from both the Monte Carlo and our analytical form with $R_{\text{mir}} = 1$ m, $h = 7.5$ km, $t_{\text{gate}} = 5 \mu\text{s}$, and $n_{\text{th}} = 2$. One finds that the Monte Carlo and the analytic methods are in good agreement. The neutrino aperture expands with energy both because of the increasing effective aperture column density for shower detection and because of the increasing interaction cross section.

Beyond HiRes, the Japanese group is planning a large array of air fluorescence and Cerenkov telescopes named the Telescope Array (Teshima et al. 1992). We estimate the expected aperture for this experiment with possible parameters of $R_{\text{mir}} = 1.5$ m and $t_{\text{gate}} = 350$ ns. It is also shown in Figure 11. Although the final configuration and speci-

cation for the Telescope Array have not been determined yet and the aperture is somewhat uncertain, we should point out that an air fluorescence detector could basically provide a neutrino detection sensitivity D_ν as high as $\sim 10^4$ m² sr at 10^{19} eV, which is determined mainly by the extinction length r_0 , the charged current cross section, and the solid angle for detection of the DPS rather than specific detector parameters like R_{mir} and t_{gate} .

The event rate for neutrino-induced showers is estimated by equation (24). Table 2 gives the expected event rate in HiRes and the Telescope Array for the possible EHE neutrino flux of the TD models. Figure 12 shows the detection probability during 10 years of running. It is found that the SCS model gives a measurable flux of neutrinos. For the ordinary cosmic string or monopole scenario, whether EHE neutrinos are detectable depends on the X-particle mass, which determines the enhancement factor of the fluxes due to neutrino cascading. If the mass of X-particles is heavier than 10^{16} GeV, we have a chance to detect EHE neutrinos with air fluorescence detectors during 10 years of observation.

An uncertainty in this estimate arises from uncertainty of the primary neutrino flux estimate (at least a factor of 2) and

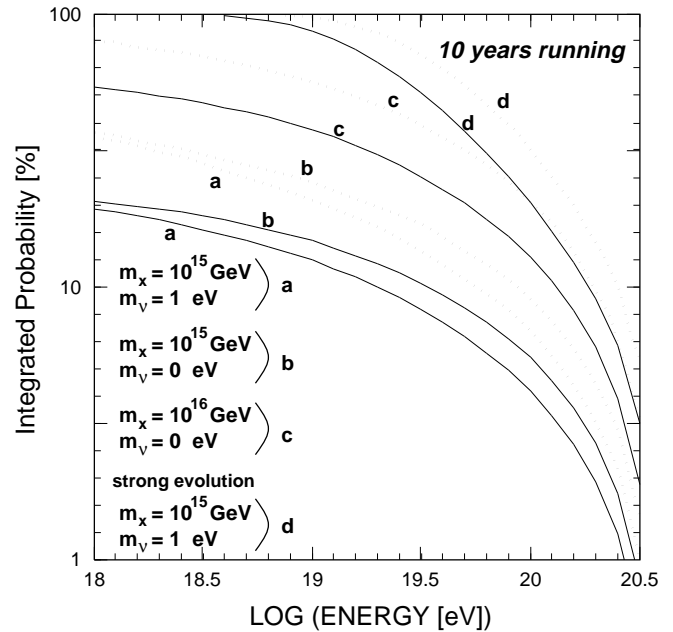


FIG. 12.—Detection probability of the EHE neutrinos during 10 years of observation by HiRes (*solid curves*) and the Telescope Array (*dotted curves*). A 10% duty cycle is taken into account. The plotted detection probability is the Poisson probability of detecting at least one neutrino shower, given the calculated expected number.

TABLE 2
EXPECTED NUMBER OF EVENTS BY HiRES (HR) AND TELESCOPE ARRAY (TA) INDUCED BY EHE NEUTRINOS FROM THE COLLAPSE OF TDS DURING A 5 YEAR EXPERIMENT

| COSMIC-RAY ENERGY | $m_x = 10^{16}$ GeV $m_\nu = 0$ eV | | $m_x = 10^{15}$ GeV $m_\nu = 0$ eV | | $m_x = 10^{15}$ GeV $m_\nu = 1$ eV | | SCS $m_\nu = 1$ eV | |
|--------------------------|---------------------------------------|------|---------------------------------------|------|---------------------------------------|------|-----------------------|------|
| | HR | TA | HR | TA | HR | TA | HR | TA |
| $E \geq 10^{18}$ eV..... | 0.38 | 0.79 | 0.11 | 0.23 | 0.11 | 0.22 | 5.93 | 15.6 |
| $E \geq 10^{19}$ eV..... | 0.23 | 0.41 | 0.08 | 0.14 | 0.07 | 0.12 | 0.99 | 1.77 |

from uncertainty in estimating cross sections for the interactions of EHE neutrinos with nucleons. Gandhi et al. (1995) recently reevaluated the cross sections based on improved knowledge of parton distributions measured by the electron-proton collider Hadron Electron Ring Accelerator (HERA). The dashed curve in Figure 10 shows their new estimate. It is larger than the calculated value based on the previous estimation (e.g., Mackey & Ralston 1986) by 20% at 1 EeV, 40% at 10 EeV, and 70% at 100 EeV. This reevaluation, however, would not significantly affect the event rates listed in Table 2, since statistical fluctuations and other uncertainties (e.g., the fragmentation spectrum equation [10]) would dominate an uncertainty due to ambiguity in the cross section.

6. BACKGROUNDS

Neutrino interactions in the atmosphere are expected to produce at most a few detections of deeply penetrating air showers over the course of a long experiment. It is therefore important to study whether other phenomena could produce similar deep showers. One possibility is a DPS resulting from the decay of an EHE tau lepton deep in the atmosphere. Another possibility is a DPS due to an EHE γ -ray bremsstrahlung by a muon. In either case, the DPS would be associated with a higher energy primary shower that produced the taus or muons. Although the primary shower may be far away, it should still be evident as an EHE shower by either its fluorescence light or its Cerenkov light. The danger of mistaking the secondary shower for a neutrino event arises only if distant clouds block all evidence of the primary shower without obscuring the DPS secondary shower.

To be conservative, we will here assume that the primary shower is *not* detected when a deep EHE shower is produced by tau decay or muon bremsstrahlung. We evaluate an approximate upper limit for the rate of detectable deep secondary showers of that type caused by cosmic-ray air showers in the atmosphere. Several factors combine to make this rate small. First of all, air shower production of EHE taus and muons is small enough that their intensities are low compared to the intensity of equal-energy primary cosmic rays. Second, they can only occur at zenith angles between 70° and 90° . Otherwise, there is not enough slant depth along the axis for the secondary shower to start deeper than 2000 g cm^{-2} and develop above ground level (taken to be at 860 g cm^{-2} vertical depth for the analysis here). Third, on these long slant shower axes, the probab-

ity is small that the secondary shower will develop within the detectable volume of atmosphere. The secondary shower is likely to start too soon or too late. Taken together, we find that these factors cause the detection rate for deeply penetrating secondary showers to be almost negligible for the detectors now being built or planned. Extremely high energy neutrino astronomy with air fluorescence detectors is limited by the signal, not by the background.

Extremely high energy taus and muons may be produced in a shower either from the weak decay of a heavy quark, from the decay of a (real or virtual) W or Z, or from Drell-Yan processes. Being weak processes, the contributions from the weak boson and Drell-Yan production are negligible compared to that from the production of heavy quarks via the strong interaction. The production rate of EHE taus and muons have therefore been estimated from $c\bar{c}$ and $b\bar{b}$ cross sections, using a first-order perturbative QCD calculation as implemented in the PYTHIA event generator (Sjöstrand 1992) and using the default fragmentation parameterization. Each produced bottom or charm particle is allowed to decay (rather than interact), and the numbers of resulting taus and muons are counted at each energy. In a realistic simulation, the hadronic cascades should be simulated along sampled trajectories through the atmosphere, and many of the bottom and charm particles would interact instead of decaying. That would degrade the bottom and charm to lower energies, and the effect would be to reduce the overall intensity of taus and muons at all energies. By allowing each produced bottom or charm particle to decay, we are overestimating the tau and muon intensities. The resulting estimate for deep secondary showers is therefore useful only as an upper limit. The true rates should be lower.

These (upper limit) intensities of taus and muons depend on the cosmic-ray spectrum. If the spectrum is a power law, then the rates depend on the spectral index and the maximum cosmic-ray energy (spectrum cutoff). The intensity is larger for flatter spectra and for larger cutoffs. Table 3 displays results for some different assumptions about the cosmic-ray differential spectral index and cutoff energy. For each case, the integral intensity of cosmic rays above 10^{19} eV is normalized to the observed value of $0.5 \text{ km}^{-2} \text{ sr}^{-1} \text{ yr}^{-1}$. It should be emphasized that the spectrum hypotheses are for the cosmic-ray spectrum at Earth, not the source spectrum. The spectral hypotheses in the table are probably unreasonably hard, in view of the pion photoproduction

TABLE 3

UPPER LIMITS FOR THE EXPECTED NUMBER OF DEEP SECONDARY SHOWERS DURING A 10 YEAR EXPERIMENT WITH 10% DUTY CYCLE (1 YEAR OF ON-TIME)

| Differential Spectral Index | Energy Cutoff (EeV) | $I_\tau/I_{\text{CR}} (E > 1 \text{ EeV})$ (Upper Limit) | $I_\mu/I_{\text{CR}} (E > 1 \text{ EeV})$ (Upper Limit) | Detectable Deep τ Showers (Upper Limit) | Detectable Deep μ Showers (Upper Limit) |
|-----------------------------|---------------------|--|---|--|---|
| 3.0 | 1000 | 7.5×10^{-8} | 2.9×10^{-7} | 2.9×10^{-4} | 3.5×10^{-7} |
| 2.0 | 1000 | 5.3×10^{-6} | 2.3×10^{-5} | 2.2×10^{-3} | 9.7×10^{-6} |
| 2.0 | 10000 | 8.2×10^{-6} | 3.7×10^{-5} | 3.4×10^{-3} | 2.6×10^{-5} |
| 1.3 | 1000 | 1.6×10^{-4} | 7.2×10^{-4} | 1.6×10^{-2} | 1.1×10^{-4} |
| 1.3 | 10000 | 7.4×10^{-4} | 3.5×10^{-3} | 6.6×10^{-2} | 8.1×10^{-4} |

NOTE.—The first two columns describe the hypothetical primary cosmic-ray spectra at Earth. The third column is the (upper limit) integral intensity of produced taus above 1 EeV, normalized by the integral intensity of primary cosmic rays. The fourth column is the corresponding quantity for muons. The last two columns give upper limits for the numbers of expected deep EHE secondary showers detected as the result of tau decays and muon bremsstrahlung, respectively.

energy losses. The tau and muon intensity upper limits would be lower for more plausible softer spectra.

For the case of a secondary tau lepton, it is also necessary to consider the probability that it will decay deep enough to be confused with a neutrino shower ($>2000 \text{ g cm}^{-2}$) but early enough for its shower development to be above ground and within the fiducial volume, which is consistent with equation (30). The probability is small for the high-energy taus. The mean decay length is 50 km at 1 EeV, 500 km at 10 EeV, etc. The probability depends on the trajectory and the tau point of production as well as the tau energy. We have numerically integrated over all viable trajectories, assuming the tau is produced at 500 g cm^{-2} slant depth. (This is deeper than expected for production of a high-energy tau. It makes the detection volume closer than expected to the tau production point, consistent with our pursuit of an upper limit.) We also assume that all of the tau's energy goes into the secondary air shower. In reality some tau decays produce only muons and neutrinos, yielding no air shower. In the other decays, at least some of the energy is taken by neutrinos, so we are also overestimating the detectable deep tau shower rate by not simulating the tau decays in detail. Results for various cosmic-rays spectra are given in Table 3. The tabulated upper limit for detected deep tau showers is for a 10 year experiment with a 10% duty cycle. Even for the hardest spectrum, the expected number of deep showers due to taus is less than 0.1.

The deep muon rates in Table 3 result from numerically integrating over possible trajectories, as in the deep tau rate calculation. In the muon case, the computation includes the probability that the muon will produce some bremsstrahlung γ -ray whose shower starts deeper than 2000 g cm^{-2} and is detectable in the fiducial volume. The expected number of deep showers due to muon bremsstrahlung is even less than what is expected from tau decays.

If a fluorescence detector experiment were expected to detect many deep secondary particle EHE air showers, then there would be concern that one or more of them might be mistaken for a neutrino event because of the primary shower being obscured by clouds. The estimates here are unrealistically high and serve only as upper limits. They show that no detections of secondary deep showers are expected. With or without clouds, therefore, there should be no such background to interfere with the identification of neutrino events.

The search for deep *secondary* showers is of interest in its own right. The estimates here show that none are expected. The detection of deep secondary showers would be evidence for an enhancement of bottom or charm production. It is therefore pertinent to search for deeply penetrating EHE subshowers which occur in association with distant primary air showers of higher energy.

7. CONCLUSIONS

We have analyzed the production of EHE neutrinos and estimated their flux based on several different models. The most certain process for producing such neutrinos—the decay of pions photoproduced by EHE cosmic rays propagating in the microwave background radiation—is not able to give rise to measurable EHE neutrino fluxes unless sources with extremely strong evolution emit EHE cosmic rays with very hard spectra. In that case the neutrino flux would exceed the cosmic-ray flux by a factor of more than

100 at around 10^{19} eV . However, it is hard to reconcile such strong evolution with deep sky X-ray and radio surveys.

An allowed mechanism that would result in copious EHE neutrinos is the annihilation or collapse of TDs such as monopoles and cosmic strings, which could also account for the highest energy cosmic-ray events recently detected well beyond 10^{20} eV . The energies of EHE neutrinos produced by this process range up to the GUT energy scale ($\sim 10^{16} \text{ GeV}$), and their interactions with cosmic background neutrinos initiate significant neutrino cascading. The cascade neutrinos enhance the flux at Earth, and we have derived the expected flux, including this enhancement factor, both for the assumption of stable massive neutrinos and for the assumption of massless neutrinos. We find that the neutrino intensities would dominate over the observed cosmic-ray intensity at 10^{19} eV by a factor of 30–100 with reasonable assumptions concerning the mass of the X-particles and neutrinos and using the expected evolution of monopoles and cosmic strings. Heavier X-particles would produce a higher neutrino flux due to increased enhancement from neutrino cascading. If neutrinos have limited mass, the Z_0 resonance effect on the neutrino cross section results in a slight suppression of the neutrino intensity at the resonance energy together with enhancement of the fluxes at lower energies. For TDs with stronger evolution such as the saturated superconducting cosmic string loops, the resonance effect would create a clear dip structure in the neutrino spectrum after propagating in a massive neutrino background. Therefore the neutrino spectrum expected from the TD scenario would contain an indicator of the neutrino mass.

The large new detectors being built to observe EHE cosmic-ray air showers by air fluorescence have the potential to detect EHE neutrinos as anomalous showers that start deep in the atmosphere. We have evaluated the sensitivity of these detectors for discovering an EHE neutrino flux. The conclusion is that one of the new cosmic-ray detectors could detect a few EHE neutrino showers during 10 years of observation if the topological defect scenario is correct. A potential background of deeply penetrating showers could arise from secondary showers that result from tau lepton decays deep in the atmosphere or from EHE γ -ray bremsstrahlung by muons. In either of these cases, it should be possible to recognize the higher energy primary shower that gave rise to the tau or muon. Such secondary showers need not be a genuine background for neutrino shower detection. Even if the primary showers were not detectable, our estimated upper limits for DPS event rates produced by high-energy secondary taus and muons are found to be more than 2 orders of magnitude lower than the neutrino event rates expected from the TD scenario. Therefore EHE neutrino astronomy with air fluorescence detectors is limited by the signal, not by the background. A search for EHE neutrinos is indeed a meaningful test of the TD hypothesis.

The authors are grateful to Guenter Sigl of the University of Chicago for his useful comments and encouragement. This work was supported in part by National Science Foundation grants PHY-9322298, PHY-9321949, PHY-9215987, and Grants-in-Aid (grant 08041094) in Scientific Research from the Japanese Ministry of Education, Science, and Culture.

REFERENCES

- Baltrusaitis, R. M., et al. 1985, *Phys. Rev. D*, 31, 2192
- Bhattacharjee, P., Hill, C. T., & Schramm, D. N. 1992, *Phys. Rev. Lett.*, 69, 567
- Bhattacharjee, P., & Sigl, G. 1995, *Phys. Rev. D*, 51, 4079
- Biermann, P. L., & Strittmatter, P. A. 1987, *ApJ*, 322, 643
- Bird, D. J. et al. 1993, *Phys. Rev. Lett.*, 71, 3401
- . 1994, *ApJ*, 424, 491
- . 1995, *ApJ*, 441, 144
- Bludman, S. A. 1992, *Phys. Rev. D*, 45, 4720
- Boyle, A. et al. 1994, *MNRAS*, 287, 373
- Chi, X., et al. 1993, *Astropart. Phys.*, 1, 239
- Dai, H. Y. 1993, in *Proc. Tokyo Workshop on Techniques for the Study of Extremely High Energy Cosmic Rays*, ed. M. Nagano (Tokyo: ICRR), 133
- Dunlop, J. A., & Peacock, J. A. 1990, *MNRAS*, 247, 19
- Elbert, J. W., & Sommers, P. 1995, *ApJ*, 441, 151
- Emerson, B. L. 1992, Ph.D. thesis, Univ. Utah
- Gaisser, T. K. 1990, *Cosmic Rays and Particle Physics*: (Cambridge: Cambridge Univ. Press), 89
- Gaisser, T. K., & Stanev, T. 1985, *Phys. Rev. D*, 31, 2770
- Gandhi, R., et al. 1995, *Astropart. Phys.*, submitted
- Greisen, K. 1956, *Prog. Cosmic Ray Phys.*, 3, 1
- . 1966, *Phys. Rev. Lett.*, 16, 748
- Hayashida, N., et al. 1994, *Phys. Rev. Lett.*, 73, 3491
- Hill, C. T., & Schramm, D. N. 1985, *Phys. Rev. D*, 31, 564
- Hill, C. T., Schramm, D. N., & Walker, T. P. 1987, *Phys. Rev. D*, 36, 1007
- HiRes collaboration. 1993, staged construction proposal for the High Resolution Fly's Eye Detector
- Kronberg, P. P. 1994, *Rep. Prog. Phys.*, 57, 325
- Lawrence, M. A., Reid, R. J. O., & Watson, A. A. 1991, *J. Phys. G: Nucl. Phys.*, 17, 733
- Mackey, D. W., & Ralston, J. P. 1986, *Phys. Lett. B*, 167, 103
- Mannheim, K. 1993, *Phys. Rev. D*, 48, 2408
- . 1995, *Astropart. Phys.*, 3, 295
- Nagano, M., et al. 1992, *J. Phys. G: Nucl. Part. Phys.*, 18, 423
- Punch, M. 1992, *Nature*, 160, 477
- Quigg, C., Reno, M. H., & Walker, T. P. 1986, *Phys. Rev. Lett.*, 57, 774
- Quinn, J., et al. 1995, *IAU Circ.* 6169 (June 16)
- Rachen, J. P., & Biermann, P. L. 1993, *A&A*, 272, 161
- Roulet, E. 1993, *Phys. Rev. D*, 47, 5247
- Sandage, A., & Cacciari, C. 1990, *ApJ*, 350, 645
- Sigl, G., Jedamzik, K., Schramm, D. N., & Berezhinsky, V. S. 1995, *Phys. Rev. D*, 52, 6682
- Sigl, G., Lee, S., & Coppi, P. 1996, *Phys. Rev. Lett.*, submitted
- Sigl, G., Schramm, D. N., & Bhattacharjee, P. 1994, *Astropart. Phys.*, 2, 401
- Sjöstrand, T. 1992, *PYTHIA 5.6 and JETSET 7.3: Physics and Manual*, CERN-TH.6488/92
- Stecker, F. W., et al. 1991, *Phys. Rev. Lett.*, 66, 2697
- . 1992, *Phys. Rev. Lett.*, 69, 2738E
- Szabo, A. P., & Protheroe, R. J. 1994, *Astropart. Phys.*, 2, 375
- Teshima, M., et al. 1992, *Nucl. Phys. B (Proc. Suppl.)*, 28B, 169
- Yoshida, S. 1994, *Astropart. Phys.*, 2, 187
- Yoshida, S., et al. 1995, *Astropart. Phys.*, 3, 105
- Yoshida, S., & Teshima, M. 1993, *Prog. Theor. Phys.*, 89, 833
- Zatsepin, G. T., & Kuźmin, V. A. 1966, *Zh. Eksp. Teor. Fiz.*, 4, 114